HHS Public Access

Author manuscript

Ann Neurol. Author manuscript; available in PMC 2016 December 13.

Published in final edited form as:

Ann Neurol. 2015 December ; 78(6): 982–994. doi:10.1002/ana.24535.

TPM3 deletions cause a hypercontractile congenital muscle stiffness phenotype

S. Donkervoort, MS CGC[1], **M. Papadaki, BSc**[#2], **JM. de Winter, MS**[#3], **MB. Neu, BS**[#1], **J. Kirschner, MD**[4], **V. Bolduc, PhD**[1], **ML. Yang, MD**[5], **MA. Gibbons, MS CGC**[6], **Y. Hu, MS**[1], **J. Dastgir, DO**[1], **ME. Leach, MSN APRN PPCNP-BC**[1,7], **A. Rutkowski, MD**[8], **AR. Foley, MD**[1], **M. Krüger, MD**[9], **EP. Wartchow, BSc**[10], **E. McNamara, BS**[11], **R. Ong, BSc**[11], **KJ. Nowak, PhD**[1], **NG. Laing, PhD**[12], **NF. Clarke, PhD**[13], **CAC. Ottenheijm, PhD**[3], **SB. Marston, MA DPhil DSc**[2], and **CG. Bönnemann, MD**[1]

[1] National Institutes of Health, Neuromuscular and Neurogenetic Disorders of Childhood Section, Bethesda, MD, USA [2] National Heart and Lung Institute, Imperial College London, London, UK [3] Department of Physiology, VU University Medical Center, Amsterdam, The Netherlands [4] Department of Neuropediatrics and Muscle Disorders, University Medical Center Freiburg, Freiburg, Germany [5] University of Colorado School of Medicine, Department of Pediatrics and Neurology, Section of Child Neurology, Aurora, CO, USA [6] University of Colorado Denver School of Medicine, Aurora, CO, USA [7] Children's National Health System, Washington DC, USA [8] Kaiser SCPMG, Cure CMD, P.O. Box 701, Olathe, KS 66051, USA [9] Department of General Pediatrics, Adolescent Medicine and Neonatology, University Medical Center Freiburg, Freiburg, Germany [10] Department of Pathology, Children's Hospital Colorado, Aurora, Colorado, USA [11] Neuromuscular Diseases Laboratory, Centre for Medical Research, Faculty of Medicine, Dentistry and Health Sciences, The University of Western Australia Crawley, WA, Australia [12] Centre for Medical Research, University of Western Australia, Harry Perkins Institute of Medical Research, QEII Medical Centre, Perth, Western Australia, Australia [13] Institute for Neuroscience and Muscle Research, The Children's Hospital at Westmead, University of Sydney, Sydney, Australia

[#] These authors contributed equally to this work.

Abstract

Objective—Mutations in *TPM3*, encoding Tpm3.12, cause a clinically and histopathologically diverse group of myopathies characterized by muscle weakness. We report two patients with novel *de novo* Tpm3.12 single glutamic acid deletions at positions ΔE218 and ΔE224, resulting in a

Corresponding author: Carsten G. Bönnemann, Corresponding author's address: National Institutes of Health, Porter Neuroscience Research Center, 35 Convent Drive, Bldg 35, Room 2A-116, Bethesda, MD 20892-3705, Corresponding author's phone and fax: phone: 301-594-5496, fax: 301-480-3365, carsten.bonnemann@nih.gov.

Author contributions

SD, NGL, NFC, CACO, SBM, CGB were responsible for the conception, design and coordination of the study. Acquisition and analysis of clinical and biopsy data was performed by JK, MLY, MAG, MEL, AR, YH, JD, MK, EPW and ARF. SD, MBN and VB performed the genetic analysis and interpretation. Permeabilized myofiber contractile performance was conducted by JMW and CACO. In vitro motility assay was performed by MP and SBM. Synthesis of tropomyosin in SF9 insect cells KJN, EM, RO. Writing of the final manuscript: SD, VB, ARF, CACO, SBM and CGB.

Potential Conflicts of Interest

There are no conflicts of interests.

significant hypercontractile phenotype with congenital muscle stiffness, rather than weakness, and respiratory failure in one case.

Methods—The effect of the Tpm3.12 deletions on the contractile properties in dissected patient myofibers was measured. We used quantitative *in vitro* motility assay (IVMA) to measure Ca^{2+}-sensitivity of thin filaments reconstituted with recombinant Tpm3.12 ΔE218 and ΔE224.

Results—Contractility studies on permeabilized myofibers demonstrated reduced maximal active tension from both patients with increased Ca^{2+} sensitivity with altered cross-bridge cycling kinetics in ΔE224 fibers. *In vitro* motility studies showed a two-fold increase in Ca^{2+}-sensitivity of the fraction of filaments motile and the filament sliding velocity concentrations for both mutations.

Interpretation—This data indicates that Tpm3.12 deletions ΔE218 and ΔE224 result in increased Ca^{2+} sensitivity of the troponin-tropomyosin complex, resulting in abnormally active interaction of actin and myosin complex. Both mutations are located in the charged motifs of the actin-binding residues of tropomyosin 3, thus disrupting the electrostatic interactions that facilitate accurate tropomyosin binding with actin necessary to prevent the on-state. The mutations destabilize the off-state and result in excessively sensitized excitation-contraction coupling of the contractile apparatus. This work expands the phenotypic spectrum of *TPM3*-related disease and provides insights into the pathophysiological mechanisms of the actin-tropomyosin complex.

INTRODUCTION

Tropomyosin 3, Tpm3.12, (α-tropomyosin slow) encoded by the *TPM3* gene (OMIM 191030), belongs to the actin-binding tropomyosin family and is a component of the sarcomeric thin filament troponin-tropomyosin complex. Tpm3.12 is predominantly expressed in type 1 (slow twitch) fibers and forms dimers of linear coiled-coil structures with Tpm2.2 (β-tropomyosin) encoded by *TPM2* and Tpm1.1 (α-tropomyosin) encoded by *TPM1*, which then bind head-to-tail providing structural stability to actin filaments.[1,2] This complex acts by regulating Ca^{2+}- dependent binding of the myosin head to the actin filament. It is an essential component in the regulation of muscle contraction by preventing binding of the myosin head when in the off-state and allowing it in the on-state, in preparation for the force generating power stroke. Mutations in *TPM3* recognized thus far result in a clinically and histopathologically heterogeneous group of neuromuscular disorders, characterized by progressive weakness and include cap myopathy,[3–5] congenital fiber type disproportion (CFTD),[6] and autosomal dominant as well as recessive nemaline myopathy,[7–10].

Mutations in *TPM2* also typically result in a phenotype of myopathy, manifesting with weakness. However, the deletion of a single lysine residue at position 7 in Tpm2.2 can manifest clinically with both muscle weakness and moderate progressive muscle contractures. Studies of this specific mutation suggest that the pathogenic mechanism underlying some tropomyosin-related disease may be due to elevated Ca^{2+} sensitivity of the contractile apparatus.[11,12] While such a mechanism had been predicted on theoretical molecular grounds to also be applicable for Tpm3.12,[13] this phenomenon had not yet been shown conclusively to be clinically relevant for Tpm3.12. [11,12]

Here we report two unrelated patients with two distinct but closely spaced *de novo* Tpm3.12 single glutamic acid deletions resulting in a marked generalized hypercontractile phenotype with very significant congenital muscle stiffness, in the absence of detectable weakness, and associated with respiratory failure in the more severely affected patient. The effect of the Tpm3.12 glutamic acid deletions was studied using *in vitro* motility assays and mechanics on permeabilized myofibers, and these deletions appear to result in impaired maximum force generation with altered cross-bridge cycling kinetics, and increased Ca^{2+} sensitivity of force. This study expands the clinical, phenotypic, and pathophysiological spectrum of *TPM3* mutations, which now join a specific *ACTA1* mutation as well as recessive αβ-crystallin (*CRYAB*) mutations as a myogenic cause for significant neonatal muscle rigidity.[14,15]

SUBJECTS/MATERIALS AND METHODS

Patient recruitment & sample collection

Two unrelated patients, one from the United States and one from Germany, were identified through their local neurologists. Medical history was obtained and clinical evaluations were performed as part of the standard neurologic evaluation. This study was approved by the Institutional Review Board of the National Institute of Neurological Disorders and Stroke, National Institutes of Health (NIH). Written informed consent was obtained from each family by a qualified investigator. DNA was obtained from blood based on standard procedures. Muscle biopsies were obtained as part of the regular clinical diagnostic testing and were evaluated by standard light and electron microscopic protocols. Banked muscle biopsy samples were transferred to the NIH for further analysis.

Genetic testing

Whole exome sequencing on blood samples obtained from Patient 1 (P1) and his parents was performed at the NIH Intramural Sequencing Center (NISC) using Illumina's TruSeq Exome Enrichment Kit and Illumina HiSeq 2000 sequencing instruments. Mutations were analyzed using GEM.app and x-browse and searched for in dbSNP, NHLBI EVS, Exac Browser or GEM.app.[16] PCR amplification of exon 6 of *TPM3* in P1, Patient 2 (P2), and their parents, was followed by Sanger sequencing on an ABI 3130x1 capillary sequencer, in forward and reverse direction.

Synthesis of tropomyosin in SF9 insect cells

The wildtype human *TPM3* cDNA sequence was amplified from reverse transcribed skeletal muscle RNA and then cloned into the BacPak8 plasmid (Clontech). The ΔE218 and ΔE224 mutations were introduced into the *TPM3* cDNA by site-directed mutagenesis. The wildtype and two mutant tropomyosin proteins were expressed in *Sf9* insect cells using the flashBAC baculovirus system (Oxford Expression Technologies). Recombinant proteins were purified using protocols based on Akkari *et al.* 2002.[17]

Quantitative in vitro motility assay

Thin filaments were reconstituted with 10nM rabbit skeletal muscle α-actin (labeled with TRITC phalloidin),[18] tropomyosin (40-60nM) and skeletal troponin (60nM) to study Ca^{2+}-regulation of filament motility by the quantitative *in vitro* motility assay previously

described.[19,20] Thin filament movement over a bed of immobilized rabbit fast skeletal muscle heavy meromyosin (100 μg/ml) was then compared in paired motility cells with wild type or mutant tropomyosin. Filament movement was recorded and analyzed as previously described,[19] yielding two parameters, the fraction of filaments moving and the speed of moving filaments. Fraction motile and sliding speed was measured over a range of Ca^{2+} concentrations to generate Ca^{2+}-activation curves as shown previously.[20–23] The temperature was set to 29 °C. EC_{50} values from replicate experiments were analyzed by paired t-test since EC_{50} has been shown to be normally distributed.[20,24]

Permeabilized myofiber contractile performance

The effect of the Tpm3.12 deletion on the contractile properties in myofibers derived from patients' muscle biopsies were measured. Myofiber bundles from frozen muscle biopsies from P1 and P2 and age-matched controls were isolated as described previously.[13,25,26] In brief, smaller sections (2×2mm) of the biopsies were isolated in liquid nitrogen. They were then placed for 24h at −20°C in 4 mL 50% glycerol/relaxing solution containing high concentrations of protease inhibitors [phenylmethylsulfonyl fluoride (PMSF), 0.5mM; leupeptin, 0.04mM; E64, 0.01mM]. Subsequently, the sections were placed on a 'roller band' for 24h at 4°C, followed by submersion in skinning solution for 24h at 4°C. Finally, the skinning solution was substituted by a glycerol/relaxing solution with lower concentrations of protease inhibitors and stored at −20°C until further use. On the day of an experiment, small strips (CSA 0.005~0.01 mm^2) were dissected from the glycerinated sections and washed thoroughly with relaxing solution. The strips were mounted using aluminum T-clips between a length motor (ASI 403A, Aurora Scientific Inc., Ontario, Canada) and a force transducer element (ASI 315C-I, Aurora Scientific Inc., Ontario, Canada) in a skinned fiber apparatus (ASI 802D, Aurora Scientific Inc., Ontario, Canada) that is mounted on an inverted microscope (Zeiss Axio Observer A1). Sarcomere length (2.5 μm) was set using a high speed VSL camera and ASI 900B software (Aurora Scientific Inc., Ontario, Canada). Six strips were analyzed for P1 (average CSA 0.01 mm^2), P2 (average CSA 0.005 mm^2) and control (average CSA: 0.006 mm^2). Fiber width and diameter was measured at three points along the fiber and the cross-sectional area (CSA) was determined assuming an elliptical cross-section. Fiber dimensions were determined using an inverted microscope (40x objective), a high-speed VSL camera with calibrated ASI 900B software (Aurora Scientific Inc., Ontario, Canada) and a custom-made prism that is mounted in the bath. Various types of bathing solutions were used during the experimental protocols: a relaxing solution (40 mM BES; 10 mM EGTA; 6.86 mM $MgCl_2$; 5.96 mM Na-ATP; 3.28 mM K-propionate; 33 mM creatine phosphate; 1 mM DTT; 0.5 mM PMSF; 0.2 mM Leupeptin; 0.05 mM E64), a pre-activating solution with low EGTA concentration (40 mM BES; 1 mM EGTA; 6.66 mM $MgCl_2$; 5.98 mM Na-ATP; 30.44 mM K-propionate; 33 mM creatine phosphate; 1 mM DTT; 0.5 mM PMSF; 0.2 mM Leupeptin; 0.05 mM E64), and activating solutions with incremental Ca^{2+} concentrations for graded Ca^{2+} response curves (40 mM BES; 10 mM $CaCO_3$-EGTA (for maximal activation); 6.64 mM $MgCl_2$; 6.23 mM Na-ATP; 2.1 mM K-propionate; 15 mM creatine phosphate; 1 mM DTT; 0.5 mM PMSF; 0.2 mM Leupeptin; 0.05 mM E64). The temperature of the bathing solutions was kept constant at 20°C using a temperature controller (ASI 825A, Aurora Scientific Inc. Ontario, Canada).

Absolute forces were normalized to the bundles' CSA to determine the maximal active tension. To determine the Ca^{2+}-sensitivity of force generation, permeabilized myofiber bundles were sequentially bathed in a relaxing solution, a pre-activation solution and solutions with pCa values ranging from 9.0 to 4.5. Steady-state forces were measured at all the Ca^{2+} concentrations, and subsequently these steady-state values were normalized to the maximal force obtained at pCa 4.5. The obtained force-pCa data were fit to the Hill equation [$Y=1/(1+10n_H(pCa-pCa_{50}))$]. Cross-bridge cycling kinetics were determined by imposing a rapid release-restretch protocol on an activated fiber based on previously reported methods.[27] The rate of tension redevelopment was obtained by fitting a bi-exponential through the force redevelopment curve. The resulting first-order rate constant k_1 reflects cross-bridge cycling kinetics and thus was used in the analyses methods.[28] A measure of active stiffness was obtained by applying small length perturbations on the myofibers, while the myofibers were being maximally activated, and fit to a linear curve through the data points. By dividing the maximal active tension by active stiffness, the force generation per cross-bridge is estimated.[29]

Myosin heavy chain isoform composition of myofibers used for contractility experiments

Since the contractile performance of muscle fibers is affected by the composition of myosin heavy chain isoforms, we used specialized SDS-PAGE to determine the myosin heavy chain isoforms present in the muscle fibers used for contractile measurements.[25] In brief, muscles fibers were denatured by boiling for 2 min. in SDS sample buffer. The stacking gel contained a 4% acrylamide concentration (pH 6.7), and the separating gel contained 7% acrylamide (pH 8.7) with 30% glycerol (v/v). The gels were run for 24h at 15°C and a constant voltage of 275V. Finally, the gels were silver-stained, scanned, and analyzed with One-D scan EX (Scanalytics Inc., Rockville, MD, USA) software (data not shown).

RESULTS

Clinical assessment identified two patients with a significant hypercontractile phenotype with marked congenital muscle stiffness

We identified two patients with a history of marked congenital muscle stiffness, which was most significant at the onset. Detailed clinical information is summarized in table 1, figure 1.

Patient 1 (P1) is a 5-year old male. Pregnancy was notable for decreased fetal movements but normal amniotic fluid level. He was born with arthrogryposis multiplex congenita with bilateral contractures of the hips, knees, and wrists. He also had bilateral hand fisting, right clubfoot deformity, unilateral hip dislocation, an inguinal hernia and generalized muscle stiffness. Neonatal course was complicated by transient respiratory distress, particularly during feeding, manifesting with an increased respiratory rate. He also had a history of low oxygen saturations and occasional grunting at rest as a neonate. He rolled from his back to his side at 6 months of age, could manipulate objects in his hands and bring some objects to his mouth by 15 months of age, and walked independently at 25 months of age. He had notable easy fatigability.

On examination at age 4 years, he had a “wooden feel” to his muscles, which were noted to be very stiff, particularity the hamstrings, the paraspinal muscles and the face muscle. He had well-defined biceps and prominent thigh muscles. There was no muscle weakness noted. Deep tendon reflexes were intact. He had good fine motor control. Active and passive range of motion was restricted at his shoulders, Achilles tendons, elbows, knees, and jaw. He walked on his toes with a stiff, shuffling gait with almost no flexion at the knees or hips appreciated (Suppl. Video 1). Due to restricted movement at these joints, he could not reach his arms above his head. He had excessive thoracic kyphosis, with a minimal scoliosis, and rigidity of the lower spine (Fig. 1 A and B). He had short stature with height below the 5th percentile, weight along the 10th percentile and head circumference along the 50th percentile.

He had a history of inappropriate sweating and was reported to be prone to “overheating” easily, particularly at night during sleep. His muscle stiffness was reported to exacerbate with movement and fatigue and improve with applying warm water to his muscles. He had a history of dysphagia and evidence of silent aspiration of liquids on videofluoroscopy. He also had a history of frequent episodes of bronchiolitis. He had been diagnosed with restrictive lung disease and uses a Cough Assist device to help improve expiratory function. A sleep study revealed evidence of hypoventilation. He has been advised to use nighttime non-invasive ventilation (NIV) in the form of bilevel positive airway pressure (BiPAP), but he could not tolerate the BiPAP mask. After the time of our examination, he received two courses of Botulinum toxin injections to the hamstrings and pectoral muscles in an effort to improve his range of motion, and he was able to reach his arms above his head and walk with more fluidity by 5 years of age. Diagnostic testing performed on P1 included an electromyography (EMG) at age 6 months of age, which was interpreted as being myopathic with denervating features. Continuous motor unit activity in the form of myotonia and myokymia were not observed.

Patient 2 (P2) is a three year-old female. The pregnancy was notable for polyhydramnios and decreased fetal movement. She was born at term and presented with severe, generalized muscle stiffness immediately after birth. Flexion muscle contractures were present in all large joints, which reportedly resulted in an inability for active or passive movements. Apparent involvement of the respiratory muscles contributed to recurrent episodes of apnea that led to the need for invasive ventilation with high inspiratory pressures (up to 40 cm H_2O). Treatment with carbamazepine, benzodiazepines, and baclofen reportedly provided no substantial benefit. Due to continuing ventilatory dependency, a tracheostomy was placed. She also had a percutaneous gastrostomy tube placed for feeding (Fig. 1C). She was discharged from the hospital at the age of five months. At the current age of 3 years, she remains fully ventilator-dependent with high inspiratory pressures (up to 25 cm H_2O). On examination, she had normal eye movements, appeared mentally alert. Muscle tone was markedly increased with absent deep tendon reflexes. She demonstrated the ability to use a standing frame, but had difficulty sitting due to apparent hyperactivity of her hip extensors.

Muscle tone reportedly reduced slightly after intramuscular injections of Botulinum toxin, and some limited voluntary movements were appreciated. She has started to use an assistive communication device. Extensive diagnostic evaluations including brain magnetic resonance

imaging (MRI), electroencephalography (EEG), and metabolic screening did not reveal any abnormalities. Serum creatine kinase (CK) levels varied between 200 and 1,000 U/L. EMG did not show evidence to myotonia or myokymia. Muscle ultrasound depicted markedly increased echogenicity of all muscles imaged but no evidence of muscle atrophy.

Exome analysis identified two novel de novo glutamic acid residue deletions in Tpm3.12

Whole exome sequencing of P1 and both biological parents followed by variant filtering for call quality and rarity yielded a heterozygous c.673-675delGAA (p.Glu224del, ΔE224) *TPM3* variant (reference NM_152263.3). Due to phenotypic similarity noted between P1 and P2, this region was Sanger sequenced in P2, revealing a heterozygous 3 base pair deletion c.657_659delAGA (p.Glu218del, ΔE218), resulting in the deletion of glutamic acid at amino acid 218 (Fig. 2A and B). Parental segregation studies for P1 and P2 were negative: the mutation was *de novo* in both patients. Neither mutation had been previously reported and neither were present in dbSNP, NHLBI EVS, Exac Browser or GEM.app.[16] Both mutations are located in highly conserved regions of *TPM3* (Fig. 2C and D).

Tpm3.12 ΔE218 and ΔE224 muscle biopsies did not show typical tropomyosin-pathology

Muscle biopsy of P1 was performed at age 17 months and was mildly myopathic in appearance without specific features. There was mild variation in fiber size and a mild type I fiber predominance (Fig. 3 A and E). NADH staining demonstrated irregular staining in some fibers resulting in some areas of clearing (Fig. G). Modified Gömöri trichrome stain demonstrated irregularities of the myofibrillar apparatus. There was no evidence of clear nemaline rods or a pattern consistent with congenital fiber-type disproportion (CFTD) (Fig. 3C, E and G). There was ultrastructural evidence of accumulation of mitochondria, increased lipid storage and Z-line streaming and broadening, which was focal, occurring in rare fibers, and spanning up to 6-7 sarcomeres maximally, seen on electron microscopy along with some sarcolemmal folding as a result of fiber atrophy (EM) (Fig. 3I).

Muscle biopsy of P2 was performed at age 3 weeks and demonstrated mild myopathic features. Findings included mild variation in fiber size and some rare basophilic fibers with centrally placed nuclei (Fig. 3B). There was mild type II fiber predominance seen on ATPase and NADH staining but no fiber-type grouping (Fig. 3F and H). Structures resembling minirods were identified on EM as well as some Z-band broadening in atrophic fibers (Fig. 3J). While clearly formed nemaline rods were not seen on modified Gömöri trichrome stain or EM, mini “miliary” rods were seen in small atrophic fibers on both modified Gömöri trichrome stain and on EM (Fig. 3D and J).

Increased Ca^{2+}-sensitivity for Tpm3.12 ΔE218 and ΔE224 by in vitro motility assay

Using the *in vitro* motility assay, the movement of synthetic thin filaments containing recombinant wild type or mutant tropomyosin (Tpm3.12 ΔE218 and ΔE224) was compared over a range of Ca^{2+} concentrations. This assay measures two parameters that are Ca^{2+}-regulated: fraction of filaments motile and sliding speed of the filaments. Ca^{2+} increased the fraction motile from 2% to 90% and the sliding speed from 1.3 to 4 μm/sec. The EC_{50} and Hill coefficient (n_H) were determined by fitting the Hill equation to the Ca^{2+}-activation curves. The mutations affected both the fraction motile and the sliding speed of the filaments

in a similar way. Thin filaments reconstituted with mutant tropomyosins showed a higher Ca^{2+}-sensitivity for both the fraction motile and the sliding speed; representative Ca^{2+} activation curves are shown in Figure 4. ΔE218 led to a 2 ½ -fold increase in Ca^{2+}-sensitivity (EC_{50} ratio ΔE218/WT = 0.40 ± 0.07, p = 0.004, n=4) for the fraction motile and a two-fold increase for the sliding speed (EC_{50} ratio ΔE218/WT = 0.48 ± 0.12, p = 0.02, n=4). ΔE224 also showed an increase in Ca^{2+}-sensitivity in both the fraction motile and the sliding speed parameter by 2.2 and 3.0-fold respectively (EC_{50} ratio ΔE224/WT for fraction motile = 0.46 ± 0.09, p = 0.01, n=4 EC_{50} ratio ΔE224/WT for sliding speed = 0.33 ± 0.08, p = 0.004, n=4), indicating that both mutations cause a gain of function. There was no significant difference in the maximum fraction motile, maximum sliding speed or Hill coefficient between either of the mutants and the wild type thin filaments.

ΔE218 and ΔE224 permeabilized myofibers showed decreased maximum force generation and ΔE218 showed increased Ca^{2+}-sensitivity with reduced cross-bridge cycling kinetics

Contractile properties of permeabilized myofibers isolated from biopsies from P1 and P2 (ΔE224 and ΔE218) were measured. The maximal active tension in ΔE218 (31 ± 5) and ΔE224 (35 ± 2) permeabilized myofibers showed a significant decrease in maximum force generation compared to controls (95 ± 14) (Fig. 5A). The Ca^{2+} sensitivity of force generation in ΔE224 (5.94 ± 0.02) was increased compared to control fibers (5.81 ± 0.02) (Fig. 5B and C). The maximum force a muscle fiber can generate is dependent on the rate of cross-bridge cycling kinetics. The rate constant of force redevelopment (*K*tr) is a widely used parameter of cross-bridge cycling kinetics, reflecting both cross-bridge attachment and detachment. Analysis showed that cross-bridge cycling kinetics are reduced in Tpm3.12 ΔE224 (6.1 ± 1) compared to control myofibers (9.8 ± 1) (Fig. 5D) while maximal active tension over active stiffness, a reflection of the force per cross-bridge, was not altered between Tpm3.12 ΔE224 (2.2 ± 0.1) and control fibers (2.2 ± 0.1) (Fig. 5E). Unfortunately, due to technical limitations caused by lower quality and quantity of the biopsy, we could not measure cross-bridge cycling kinetics and force per cross-bridge in Tpm3.12 ΔE218.

As the contractile performance of myofibers is dependent on the myosin heavy chain (MHC) isoform composition, the presence of MHC isoforms was determined. No significant changes between control myofibers (27 ± 6% slow MHC and 73 ± 6% fast MHC) and ΔE218 (30 ± 5% slow MHC and 66 ± 6% fast MHC) or ΔE224 (20 ± 7% slow MHC and 80 ± 7% fast MHC) were found. Therefore, the changes observed in contractile performance between control and patient myofibers were not influenced by changes in myosin heavy isoform composition, and are more likely due to the specific mutations.

DISCUSSION

Muscle fiber based stiffness, in the absence of clinically detectable weakness, is a rare manifestation of congenital muscle disease. It was originally reported in Canadian aboriginal patients with a fatal condition characterized by progressive muscle stiffness and respiratory insufficiency[15] due to recessive mutations in *CRYAB*. *CRYAB* codes for the small chaperone αβ-crystalline; however, the mechanism responsible for the muscle stiffness remains unclear. Additionally, a specific *de novo* mutation in *ACTA1* was found in a

newborn with congenital episodic stiffness, hypertrophic muscles and nemaline rod muscle pathology.[14] Our report is the first to demonstrate specific *TPM3* deletions as the cause of a novel phenotypic manifestation of marked and generalized congenital muscle stiffness. This phenotype is notable for an absence of muscle weakness in combination with muscle stiffness, so severe that it can result in early ventilatory failure, likely due to an inability of respiratory muscle relaxation, as evidenced by the high inspiratory pressures required during mechanical ventilation in P2.

The muscle thin filament is a cooperative-allosteric system. Its basic unit consists of a backbone of actin monomers, the troponin-tropomyosin complex and nebulin.[24] Muscle contraction is regulated by Ca^{2+} via its release and reuptake from the sarcoplasmic reticulum. Ca^{2+} binding to troponin C on the thin filaments of muscle results in switching contraction from the “off” to the “on” state by causing a sideward shift of the actin-binding tropomyosin dimer, exposing the myosin binding site on the actin filament.[30–32] Tropomyosins thus play a vital role in transmitting the Ca^{2+} signal from the troponin to the actin myosin binding site. Mutations in *TPM3* (coding for Tpm3.12) are an established molecular cause of a clinically and histopathologically heterogeneous group of myopathies, characterized by progressive weakness and by variable but characteristic findings on muscle pathology including nemaline rods, CFTD or cap-like structures. The phenotype associated with Tpm3.12 ΔE218 and ΔE224, with its congenital stiffness resulting from marked muscle hypercontractility, is significantly different from these known manifestation of *TPM3*-related disease. Muscle biopsies analysis did not reveal the typical muscle pathology seen in tropomyosin-related disease, including clear nemaline rods, although small rod-like structures (“miliary rods”) were seen in atrophic fibers of P1. We also found evidence of myofiber damage histologically, likely due to the permanently hypercontracted state of the muscle fibers, consistent with increased CK values. Six *TPM2* and one *TPM3* mutation that result in increased Ca^{2+}-sensitivity have been reported in patients with only moderately progressive contractures and myopathic weakness.[11,12,33]In contrast, our patients present with a distinctive and considerably more severe congenital hypercontractile phenotype with generalized muscle stiffness leading to severe respiratory failure in the neonatal period in one case, which represents a novel phenotype for tropomyosin-related disease.

Mutations in tropomyosin or actin that produce a hypercontractile phenotype may destabilize the “switched off” state, shifting the equilibrium in favor of the “switched on” state of actin-tropomyosin which allows for myosin binding, thereby increasing Ca^{2+}-sensitivity and, in one case, increasing maximum force generated and cross bridge cycling rate.[11,14,34,35] The finding that the Tpm3.12 ΔE218 and ΔE224 mutations introduced into recombinantly expressed tropomyosin resulted in increased Ca^{2+}-sensitivity in the *in vitro* motility assay (Fig. 4), and that the Tpm3.12 ΔE224 biopsy has increased Ca^{2+}-sensitivity of force production (Fig. 5) is compatible with this mechanism as the basis of the hypercontractile phenotype.

The hypercontractile phenotype associated with these Tpm3.12 mutations also conforms to the predictions made by Marston et al.[22] on biophysical grounds (Fig. 6), which we now confirm clinically as well as *in vitro*. The atomic resolution structure of tropomyosin-bound actin shows that tropomyosin makes contact with actin at only two points: with actin Asp25

and with a cluster of basic amino acids actin K326, K328 and R147.[36] Tropomyosin has a seven-fold repeated structure corresponding to seven actin-binding interactions. Three Tpm2.2 mutations and the Tpm3.12 mutation K169E were shown to destabilize the interaction with actin Asp25, based on energy landscape calculations, and increase Ca^{2+}-sensitivity in *in vitro* motility assay, consistent with gain of contractile function.[22,37] More importantly, two Tpm2.2 mutations, ΔE139 and E181K, destabilize the interaction with the actin K326, K328, and R147 cluster. All of these mutations involve a charge loss or reversal in a motif of two basic or acidic amino acids. There are nine such motifs in all tropomyosin isoforms. Mutations have been described in myopathy patients with increased *in vitro* Ca^{2+}-sensitivity for six of the nine motifs (five in Tpm2.2 and one in Tpm3.12, three of which were associated with a phenotype of arthrogryposis or some signs of stiffness or contractures in addition to weakness). The remaining three motifs are at 218-219, 224-224 (EE), and 257-258 (ED) in either tropomyosin.[22] Thus, the “stiff” patients’ mutations reported here are in the first two of these three remaining domains, which were predicted to result in a hypercontractile state. It is striking that the hypercontractile consequences in our cases are clinically more pronounced compared to the manifestations of other tropomyosin mutations previously reported. Notably, most of the mutations tested *in vitro* and found to display increased Ca^{2+}-sensitivity are located adjacent to the tropomyosin amino acid that interacts with actin rather than at the site itself.[22] This also applies to Tpm3.12 E218 and E224, which do not interact with actin, whilst neighboring Tpm3.12 E219 and E223 interact directly with the actin K326, K328, and R147 cluster (Fig. 6). In light of the structural analysis modeling of these physical interactions, it is significant that the actin K326N mutation at the cognate site in actin itself was the first “stiff” patient mutation reported in a thin filament protein.[14,22,38] The degree of stiffness seen in that patient appeared similar to our observation.[14]

The *in vitro* sliding data obtained with mutant protein provide the crucial link to understanding the clinical hypercontractile phenotype; however, the consequences of the mutation on the entire thin filament and contractile fiber show additional complexities. Notably, the skinned fiber preparation had decreased maximal active tension resulting in a decrease in maximal force generation, while the force per cross bridge was not altered. This raises the possibility that the cycling of cross bridges back into the “off” state is impaired. The observed reduction in rate constant of force redevelopment, which indicates a reduced effectiveness of cross bridge cycling, could explain the impaired force generation capacity of the muscle. Muscle fibers from P1 (ΔE224) generated a higher relative force at the same Ca^{2+} concentration, which may therefore compensate for the loss of maximal force-generating capacity. Since there was no evidence of weakness in the patients (at the time of examination), we surmise that the hypercontractility at submaximal calcium concentrations is so overwhelming that any decrease in maximal force does not come to bear on the phenotype. The continuous cellular stress of the hypercontractility of the muscle may cause future muscle damage and breakdown in our patients, possibly resulting in weakness and findings of tropomyosin muscle pathology over time. That this is indeed occurring is suggested by the CK elevations and also by the markedly abnormal muscle ultrasound findings in P2.

The question remains as to why the stiffness phenotype in our patients is significantly more severe and generalized compared to the best characterized gain of function mutation in Tpm2.2, the ΔK7 deletion, identified in patients with progressive, early-onset contractures without clear muscle weakness in childhood but with some stiffness noted in one 14-year-old boy.[11] Tpm2.2 is expressed in both fast and slow-twitch fibers. Increased Ca^{2+}-sensitivity of force generation has also been observed in patients with distal arthrogryposis caused by mutations in troponin I (*TNNI2)* and troponin T3 (*TNNT3)*, encoding for contractile apparatus proteins specific to fast-twitch fibers.[40] Contractures of the distal muscles, which are predominantly fast-twitch fibers, typically develop prenatally but have little to no progression over time with relative normal proximal muscle strength and histology.[41] The generalized and more severe congenital stiffness observed in the Tpm3.12 ΔE218 and ΔE224 patients may thus be partially related to the expression pattern, with Tpm3.12 being the most relevant tropomyosin for all slow-twitch fibers.

Finally, we considered how the molecular mechanisms reported here could inform a rational therapeutic approach to these patients. P1 showed improvement with Botulinum toxin injections leading to increased range of motion, improved gait, and increased jaw mobility with enhanced speech production. Decreased neuromuscular transmission from the Botulinum application would lead to less activation of excitation-contraction coupling, likely taking the edge off the baseline hypercontractility associated with the underlying *TPM3* mutation. Given the growing amount of literature supporting changed Ca^{2+}-sensitivity of the actin-tropomyosin complex as a mechanism for muscle disease, future therapeutic strategies may involve reducing the release of Ca^{2+} at the sarcomere. An alternative approach would be to desensitize the thin filament to Ca^{2+}. In cases of decreased Ca^{2+}-sensitivity, compounds that act as Ca^{2+} sensitizers, which are under active development in the neuromuscular and heart failure field may be utilised.[40,41] The latter type of approach would likely be detrimental in the patients reported here.

In conclusion, in this study we identified two patients with a marked congenital hypercontractile phenotype caused by dominantly acting *de novo* mutations in Tpm3.12, ΔE218 and ΔE224, representing the most severe tropomyosin-related hypercontractile phenotype recognized to date. Our experiments confirm a mechanism of increased Ca^{2+}-sensitivity by which Tpm3.12 mutant muscle fibers contract at lower Ca^{2+} concentrations compared to wild type fibers. Our data lend *in vivo* and *in vitro* support to the conclusion that the increased Ca^{2+}-sensitivity observed for both ΔE218 and ΔE224 results from a destabilization of the “off” state of the thin filament, resulting in excessively sensitized excitation-contraction coupling of the contractile apparatus, as previously predicted for ΔE218 on theoretical biophysical grounds. Mutations in tropomyosin, specifically in *TPM3*, should therefore be considered when evaluating a patient with congenital-onset muscle stiffness.

Supplementary Material

Refer to Web version on PubMed Central for supplementary material.

Acknowledgements

We would like to thank NIH Intramural Sequencing Center for performing the exome sequencing. We would also like to thank the Analytic and Translational Genetics Unit (ATGU) at Massachusetts General Hospital (MGH) and Genomes Management Application at University of Miami Miller School of Medicine for their help in the exome analysis. The authors would like to thank the Exome Aggregation Consortium and the groups that provided exome variant data for comparison. A full list of contributing groups can be found at http://exac.broadinstitute.org/about. NGL was supported by Australian National Health and Medical Research Council (NH&MRC) Fellowship APP1002147, KJN by Australian Research Council Future Fellowship FT100100734 and EM and RO by NH&MRC project grant APP1022707. SBM and MK were supported by grants from the British Heart Foundation (RG/11/20/29266 and FS/12/24/29568).

REFERENCES

1. Perry SV. Vertebrate tropomyosin: Distribution, properties and function. J. Muscle Res. Cell Motil. 2001; 22:5–49. [PubMed: 11563548]
2. Murakami K, Stewart M, Nozawa K, et al. Structural basis for tropomyosin overlap in thin (actin) filaments and the generation of a molecular swivel by troponin-T. Proc. Natl. Acad. Sci. U. S. A. 2008; 105:7200–7205. [PubMed: 18483193]
3. De Paula AM, Franques J, Fernandez C, et al. A TPM3 mutation causing cap myopathy. Neuromuscul. Disord. 2009; 19:685–688. [PubMed: 19553118]
4. Ohlsson M, Fidzianska A, Tajsharghi H, Oldfors A. TPM3 mutation in one of the original cases of cap disease. Neurology. 2009; 72(22):1961–3. [PubMed: 19487656]
5. Schreckenbach T, Schröder JM, Voit T, et al. Novel TPM3 mutation in a family with cap myopathy and review of the literature. Neuromuscul. Disord. 2014; 24(2):117–24. [PubMed: 24239060]
6. Clarke NF, Kolski H, Dye DE, et al. Mutations in TPM3 are a common cause of congenital fiber type disproportion. Ann. Neurol. 2008; 63(3):329–37. [PubMed: 18300303]
7. Laing NG, Wilton SD, Akkari PA, et al. A mutation in the alpha tropomyosin gene TPM3 associated with autosomal dominant nemaline myopathy NEM1. Nat. Genet. 1995; 10(2):249. [PubMed: 7663526]
8. Tan P, Briner J, Boltshauser E, et al. Homozygosity for a nonsense mutation in the alpha-tropomyosin slow gene TPM3 in a patient with severe infantile nemaline myopathy. Neuromuscul. Disord. 1999; 9(8):573–9. [PubMed: 10619715]
9. Wattanasirichaigoon D, Swoboda KJ, Takada F, et al. Mutations of the slow muscle alpha-tropomyosin gene, TPM3, are a rare cause of nemaline myopathy. Neurology. 2002; 59(4):613–7. [PubMed: 12196661]
10. Lehtokari V-L, Pelin K, Donner K, et al. Identification of a founder mutation in TPM3 in nemaline myopathy patients of Turkish origin. Eur. J. Hum. Genet. 2008; 16(9):1055–61. [PubMed: 18382475]
11. Mokbel N, Ilkovski B, Kreissl M, et al. K7del is a common TPM2 gene mutation associated with nemaline myopathy and raised myofibre calcium sensitivity. Brain. 2013; 136(Pt 2):494–507. [PubMed: 23378224]
12. Davidson AE, Siddiqui FM, Lopez MA, et al. Novel deletion of lysine 7 expands the clinical, histopathological and genetic spectrum of TPM2-related myopathies. Brain. 2013; 136(Pt 2):508–21. [PubMed: 23413262]
13. Ottenheijm CAC, Lawlor MW, Stienen GJM, et al. Changes in cross-bridge cycling underlie muscle weakness in patients with tropomyosin 3-based myopathy. Hum. Mol. Genet. 2011; 20(10):2015–25. [PubMed: 21357678]
14. Jain RK, Jayawant S, Squier W, et al. Nemaline myopathy with stiffness and hypertonia associated with an ACTA1 mutation. Neurology. 2012; 78(14):1100–3. [PubMed: 22442437]
15. Del Bigio MR, Chudley AE, Sarnat HB, et al. Infantile muscular dystrophy in Canadian aboriginals is an αB-crystallinopathy. Ann. Neurol. 2011; 69(5):866–71. [PubMed: 21337604]
16. Gonzalez MA, Lebrigio RFA, Van Booven D, et al. GEnomes Management Application (GEM.app): a new software tool for large-scale collaborative genome analysis. Hum. Mutat. 2013; 34(6):842–6. [PubMed: 23463597]

17. Akkari PA, Song Y, Hitchcock-DeGregori S, et al. Expression and biological activity of Baculovirus generated wild-type human slow alpha tropomyosin and the Met9Arg mutant responsible for a dominant form of nemaline myopathy. Biochem. Biophys. Res. Commun. 2002; 296(2):300–4. [PubMed: 12163017]
18. Kron SJ, Toyoshima YY, Uyeda TQ, Spudich JA. Assays for actin sliding movement over myosin-coated surfaces. Methods Enzymol. 1991; 196:399–416. [PubMed: 2034132]
19. Marston SB, Fraser ID, Bing W, Roper G. A simple method for automatic tracking of actin filaments in the motility assay. J. Muscle Res. Cell Motil. 1996; 17(4):497–506. [PubMed: 8884604]
20. Messer AE, Jacques AM, Marston SB. Troponin phosphorylation and regulatory function in human heart muscle: dephosphorylation of Ser23/24 on troponin I could account for the contractile defect in end-stage heart failure. J. Mol. Cell. Cardiol. 2007; 42(1):247–59. [PubMed: 17081561]
21. Bayliss CR, Jacques AM, Leung M-C, et al. Myofibrillar Ca(2+) sensitivity is uncoupled from troponin I phosphorylation in hypertrophic obstructive cardiomyopathy due to abnormal troponin T. Cardiovasc. Res. 2013; 97(3):500–8. [PubMed: 23097574]
22. Marston S, Memo M, Messer A, et al. Mutations in repeating structural motifs of tropomyosin cause gain of function in skeletal muscle myopathy patients. Hum. Mol. Genet. 2013; 22(24): 4978–87. [PubMed: 23886664]
23. Memo M, Leung M-C, Ward DG, et al. Familial dilated cardiomyopathy mutations uncouple troponin I phosphorylation from changes in myofibrillar Ca^{2+} sensitivity. Cardiovasc. Res. 2013; 99(1):65–73. [PubMed: 23539503]
24. Fraser ID, Marston SB. In vitro motility analysis of actin-tropomyosin regulation by troponin and calcium. The thin filament is switched as a single cooperative unit. J. Biol. Chem. 1995; 270(14): 7836–41. [PubMed: 7713874]
25. Ottenheijm CAC, Witt CC, Stienen GJ, et al. Thin filament length dysregulation contributes to muscle weakness in nemaline myopathy patients with nebulin deficiency. Hum. Mol. Genet. 2009; 18(13):2359–69. [PubMed: 19346529]
26. Ottenheijm CAC, Hooijman P, DeChene ET, et al. Altered myofilament function depresses force generation in patients with nebulin-based nemaline myopathy (NEM2). J. Struct. Biol. 2010; 170(2):334–43. [PubMed: 19944167]
27. Malfatti E, Lehtokari V-L, Böhm J, et al. Muscle histopathology in nebulin-related nemaline myopathy: ultrastrastructural findings correlated to disease severity and genotype. Acta Neuropathol. Commun. 2014; 2:44. [PubMed: 24725366]
28. Caremani M, Dantzig J, Goldman YE, et al. Effect of inorganic phosphate on the force and number of myosin cross-bridges during the isometric contraction of permeabilized muscle fibers from rabbit psoas. Biophys. J. 2008; 95(12):5798–808. [PubMed: 18835889]
29. Manders E, Bogaard H-J, Handoko ML, et al. Contractile dysfunction of left ventricular cardiomyocytes in patients with pulmonary arterial hypertension. J. Am. Coll. Cardiol. 2014; 64(1):28–37. [PubMed: 24998125]
30. Gordon AM, Homsher E, Regnier M. Regulation of contraction in striated muscle. Physiol. Rev. 2000; 80(2):853–924. [PubMed: 10747208]
31. Behrmann E, Müller M, Penczek PA, et al. Structure of the rigor actin-tropomyosin-myosin complex. Cell. 2012; 150(2):327–38. [PubMed: 22817895]
32. Li XE, Tobacman LS, Mun JY, et al. Tropomyosin position on F-actin revealed by EM reconstruction and computational chemistry. Biophys. J. 2011; 100(4):1005–13. [PubMed: 21320445]
33. Marttila M, Lehtokari VL, Marston S, et al. Mutation Update and Genotype-Phenotype Correlations of Novel and Previously Described Mutations in TPM2 and TPM3 Causing Congenital Myopathies. Hum. Mutat. 2014; 35(7):779–790. [PubMed: 24692096]
34. Ochala J, Gokhin DS, Pénisson-Besnier I, et al. Congenital myopathy-causing tropomyosin mutations induce thin filament dysfunction via distinct physiological mechanisms. Hum. Mol. Genet. 2012; 21(20):4473–85. [PubMed: 22798622]

35. Memo M, Marston S. Skeletal muscle myopathy mutations at the actin tropomyosin interface that cause gain- or loss-of-function. J. Muscle Res. Cell Motil. 2013; 34(3-4):165–9. [PubMed: 23719967]

36. Orzechowski M, Li XE, Fischer S, Lehman W. An atomic model of the tropomyosin cable on F-actin. Biophys. J. 2014; 107(3):694–9. [PubMed: 25099808]

37. Orzechowski M, Fischer S, Moore JR, et al. Energy landscapes reveal the myopathic effects of tropomyosin mutations. Arch. Biochem. Biophys. 2014; 564:89–99. [PubMed: 25241052]

38. Orzechowski M, Moore JR, Fischer S, Lehman W. Tropomyosin movement on F-actin during muscle activation explained by energy landscapes. Arch. Biochem. Biophys. 2014; 545:63–8. [PubMed: 24412204]

39. Mokbel N, Ilkovski B, Kreissl M, et al. K7del is a common TPM2 gene mutation associated with nemaline myopathy and raised myofibre calcium sensitivity. [Internet]. Brain. 2013; 136(Pt 2): 494–507. [2015 Feb 10] Available from: http://www.ncbi.nlm.nih.gov/pubmed/23378224. [PubMed: 23378224]

40. Robinson P, Lipscomb S, Preston LC, et al. Mutations in fast skeletal troponin I, troponin T, and beta-tropomyosin that cause distal arthrogryposis all increase contractile function. FASEB J. 2007; 21(3):896–905. [PubMed: 17194691]

41. Sung SS, Brassington A-ME, Grannatt K, et al. Mutations in genes encoding fast-twitch contractile proteins cause distal arthrogryposis syndromes. Am. J. Hum. Genet. 2003; 72:681–690. [PubMed: 12592607]

42. Perrone SV, Kaplinsky EJ. Calcium sensitizer agents: a new class of inotropic agents in the treatment of decompensated heart failure. Int. J. Cardiol. 2005; 103(3):248–55. [PubMed: 16098385]

43. De Winter JM, Buck D, Hidalgo C, et al. Troponin activator augments muscle force in nemaline myopathy patients with nebulin mutations. J. Med. Genet. 2013; 50(6):383–92. [PubMed: 23572184]

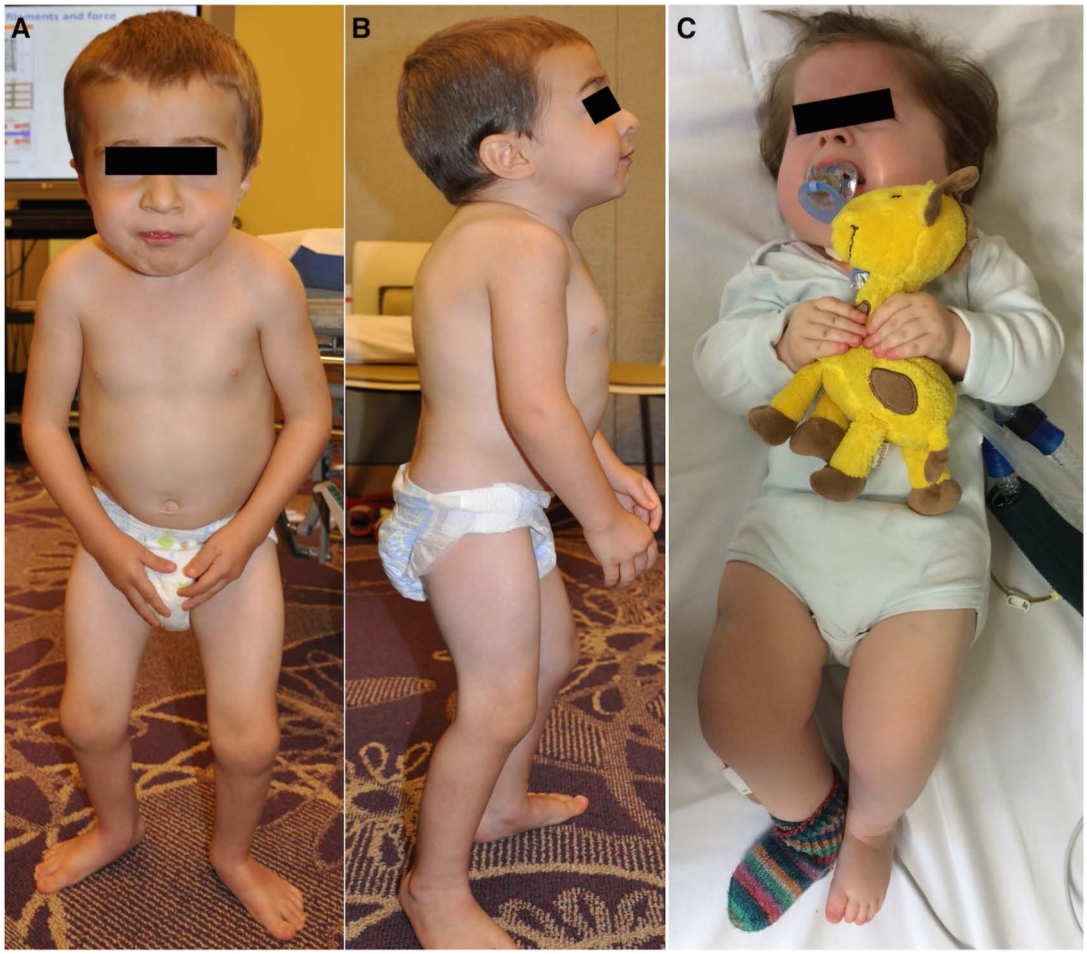

Figure 1.

(A and B). 4 year old male (P1) with relative macrocephaly compared to his short stature and thin habitus. He has a prominent forehead, small mouth, short neck and stiff face. His shoulders are anteriorly rotated with decreased lumbar lordosis and increased kyphosis and he has bilateral elbow and knee contractures. He has flat feet that are turned outwards, external hip rotation and a barrel chest with wide spaced nipples. (C). 3-year-old female (P2) with pronounced muscle stiffness. She has bilateral contractures of elbows, knees and ankles. She is ventilated with tracheostomy and has a feeding tube.

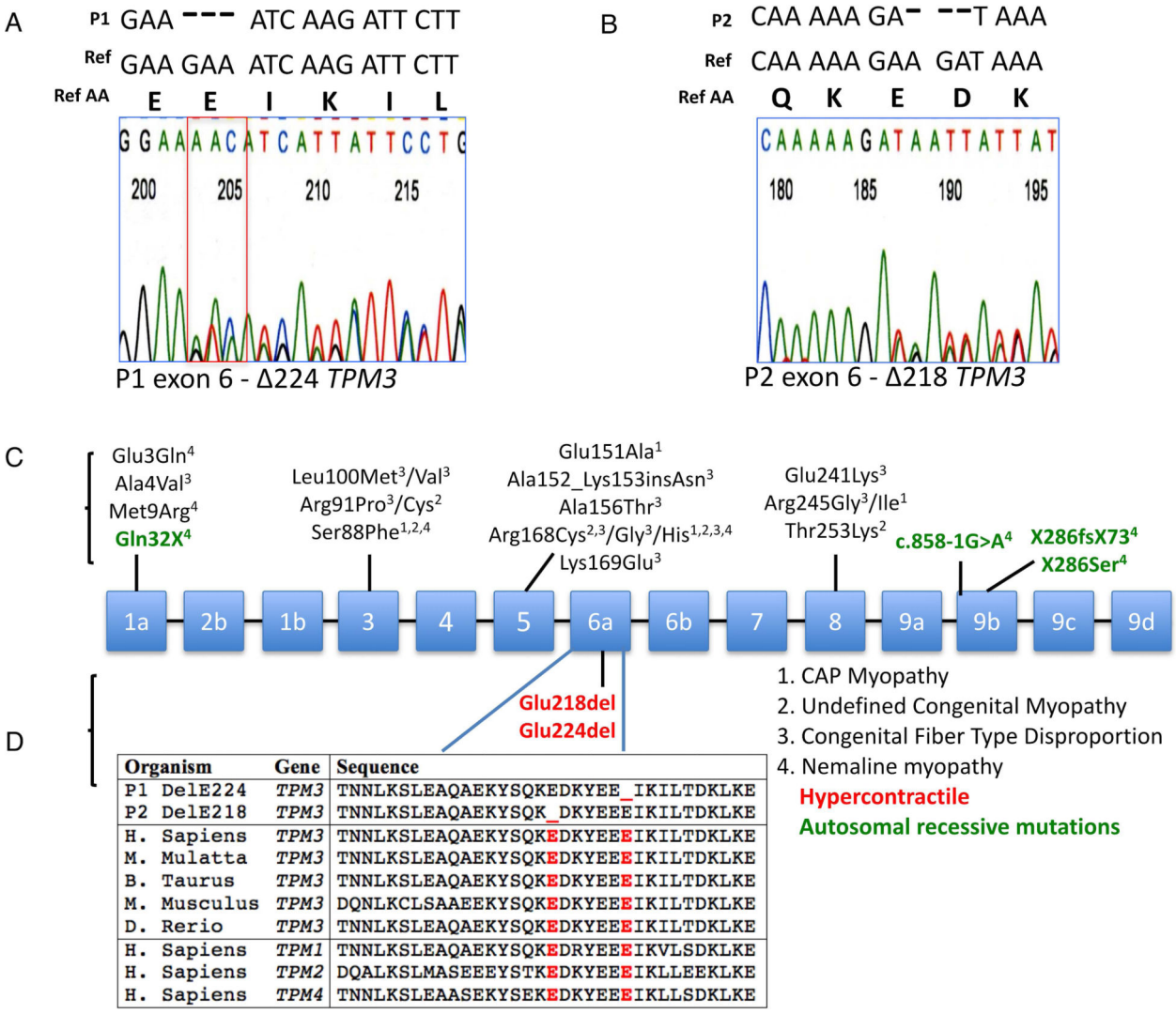

Organism	Gene	Sequence
P1 DelE224	*TPM3*	TNNLKSLEAQAEKYSQKEDKYEE_IKILTDKLKE
P2 DelE218	*TPM3*	TNNLKSLEAQAEKYSQK_DKYEEEIKILTDKLKE
H. Sapiens	*TPM3*	TNNLKSLEAQAEKYSQKEDKYEEEIKILTDKLKE
M. Mulatta	*TPM3*	TNNLKSLEAQAEKYSQKEDKYEEEIKILTDKLKE
B. Taurus	*TPM3*	TNNLKSLEAQAEKYSQKEDKYEEEIKILTDKLKE
M. Musculus	*TPM3*	DQNLKCLSAAEEKYSQKEDKYEEEIKILTDKLKE
D. Rerio	*TPM3*	TNNLKSLEAQAEKYSQKEDKYEEEIKILTDKLKE
H. Sapiens	*TPM1*	TNNLKSLEAQAEKYSQKEDRYEEEIKVLSDKLKE
H. Sapiens	*TPM2*	DQALKSLMASEEEYSTKEDKYEEEIKLLEEKLKE
H. Sapiens	*TPM4*	TNNLKSLEAASEKYSEKEDKYEEEIKLLSDKLKE

Figure 2.

Sequence chromatogram of P1 & P2 identifying a glutamic acid deletion in Tpm3.12. (A and B). Schematic of known mutations in *TPM3* along with their disease phenotypes (C). Illustration of amino acid homology of *TPM3*, P1, P2 as well as for *TPM1*, *2* & *4* (D).

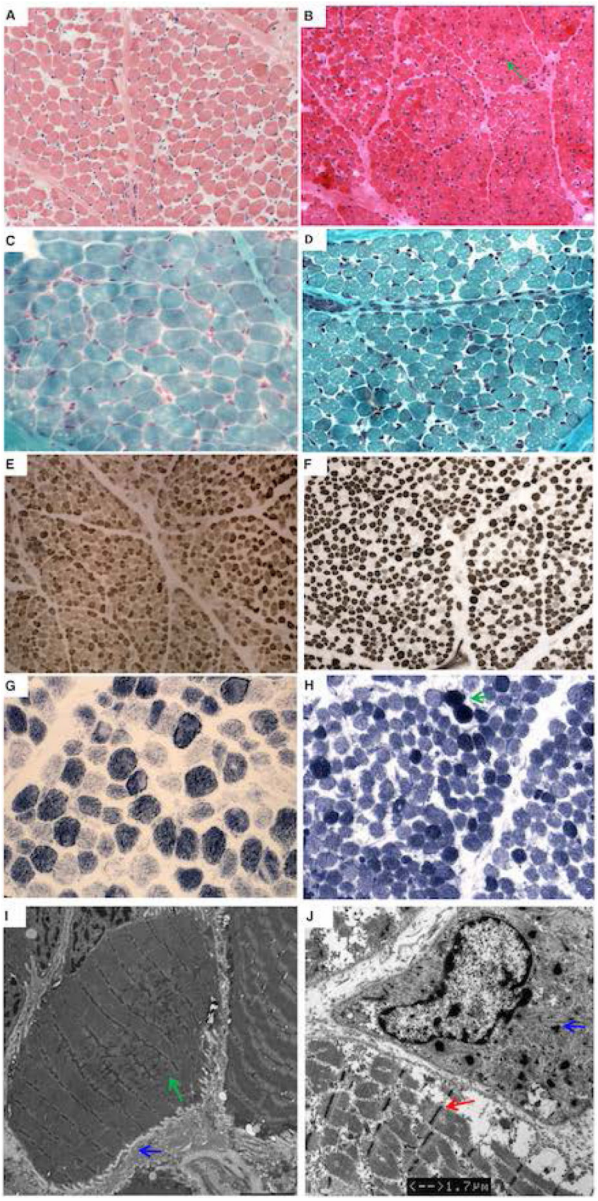

Figure 3.

Muscle biopsy of P1 at age 17 months *(left)* and P2 at age 22 days *(right)*. H&E at (at 20x) shows variability in fiber size with increased perimysial and endomysial fibrosis in P1 (A) and P2 (B). There are some rare basophilic fibers in P2 (B) with centrally placed nuclei (green arrow). Trichrome staining (at 40x) does not show inclusions suggestive of nemaline rods or vacuoles in P1 (C) while P2 shows "miliary" rod-like inclusions in some of the atrophic fibers (D). There is variation in fiber size of both fiber types on ATPase 9 (at 20x) in P1 (E) and ATPase 10.5 (at 20x) in P2 (F). There is mild type 1 predominance in P1 and mild type 2 fiber predominance in P2. NADH (at 40x) in P1 (G) and P2 (H) shows a decrease in staining in the periphery of some of the darker (type I) fibers, evidence of mitochondrial aggregation and contracted fibers (green arrow). EM of P1 shows and atrophic muscle fiber with Z-disk streaming (green arrow) and sarcolemmal folds (blue

arrow) (I) (bar = 4 μm). EM of P2 also shows Z-band broadening in an atrophic fiber (red arrow) (bar = 1.7 μm). There are some “miliary” rods (blue arrow). No clear nemaline rods were seen (J).

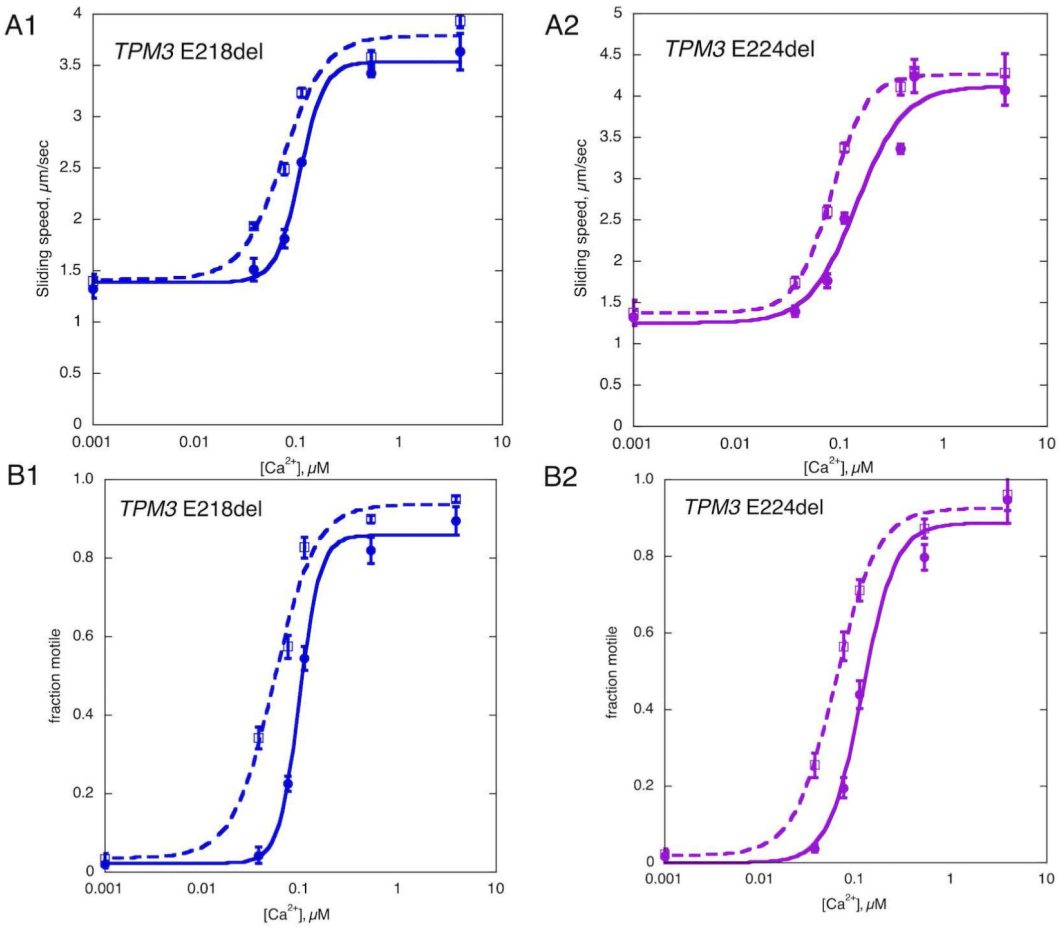

Figure 4.

Ca^{2+} control of *in vitro* motility. Representative Ca^{2+}-activation curves; ΔE218 left and ΔE224 on right compared with wild-type control. Thin filaments were assembled using baculovirus expressed Tpm3.12, rabbit skeletal muscle actin and rabbit skeletal muscle troponin. Thin filament movement over immobilized HMM was tracked and analyzed over a range of Ca^{2+} concentrations. Solid lines, control; dotted lines mutant tropomyosin. Error bars are SD for 4 measurements of motility in the same motility cell. The curves are the fits of the data to the Hill equation; sliding speed (top) and fraction of filaments motile parameters (bottom). Four separate Ca^{2+}-curves were determined for each mutation. For WT and ΔE218 EC_{50} for fraction motile were 0.20±0.06 and 0.07±0.02 respectively, for sliding speed 0.22±0.08 and 0.08±0.01 respectively. For WT and ΔE224 EC_{50} for fraction motile were 0.19±0.05 and 0.07±0.021 respectively, for sliding speed 0.30±0.08 and 0.09±0.02 respectively.

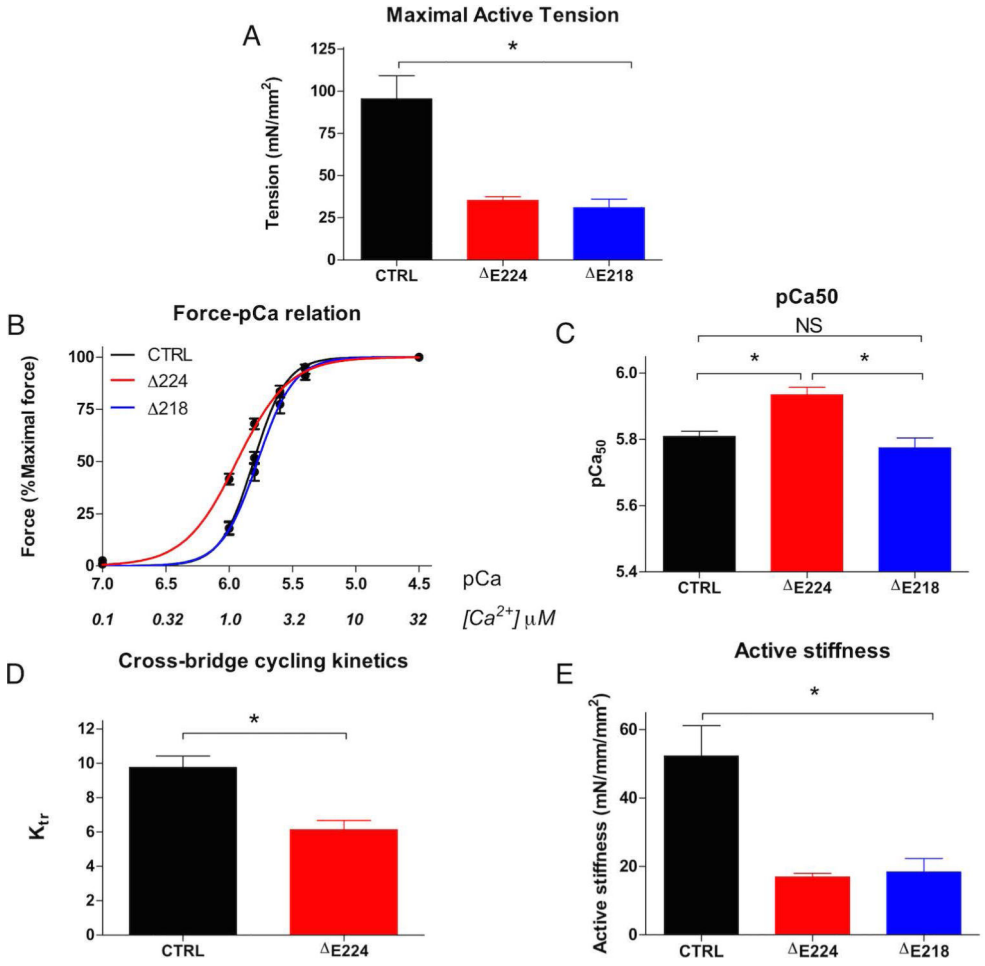

Figure 5.

A significant decrease in maximum force generation was seen in single fiber myofibres from Tpm3.12 ΔE224 & ΔE218 compared to controls (A). The Ca^{2+} sensitivity of force generation was increased in ΔE224 compared to controls and ΔE218 (B and C). Additionally there is reduced cross-bridge cycling kinetics in Tpm3.12 ΔE224 (D) while the active stiffness was not altered between Tpm3.12 ΔE224 and control (E).

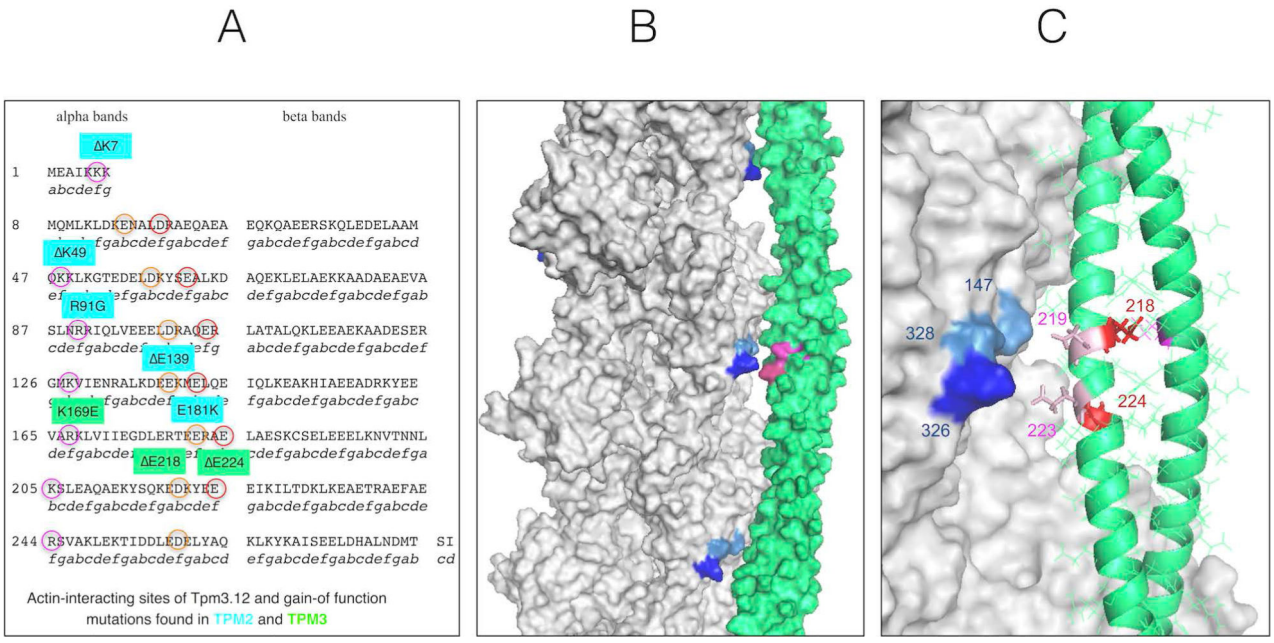

Figure 6.

Location of gain-of function mutations in tropomyosin isoforms Tpm2.2 and Tpm3.12. The amino acids predicted to interact with actin are circled (A). Structure of the F-actin-tropomyosin complex determined by Li et al (2011). Surface rendering using PyMol. Actin K326, K328 and R147 are shown in different shades of blue and tropomyosin 218,219 223 and 224 are shown in magenta (B). The interface of tropomyosin period 6 with actin. Actin K326, K328 and R147 are shown in different shades of blue, E214 and E224 in red and 219 and 223 are shown in pink. Actin is represented by surface rendering; the secondary structure of tropomyosin backbone (coiled-coil alpha helix) is shown with the side chains in line notation (C).

Table 1

Clinical details of P1 and P2.

	Patient 1 (P1)	**Patient 2 (P2)**
Sex/age (years)	Male/4	Female/3
Tpm3.12 mutation	ΔE224	ΔE218
Presentation	Decreased fetal movements. At birth: stiffness with arthrogryposis multiplex congenital, right clubfoot, bilateral hand fisting, inguinal hernia, bilateral hip dysplasia, and knee contractures.	At birth: pronounced generalized stiffness, limited to absent movement, including the thoracic muscles requiring ventilation, hip dysplasia, umbilical hernia, left inguinal hernia. In infancy: recurrent hypoxic crises.
Dysmorphic features	Relative macrocephaly, short stature, and thin habitus. Prominent forehead, small mouth, short neck, and stiff face.	Retrognathia, micrognathia, and short neck.
Cognition	Normal	Normal
Clinical features	Kyphoscoliosis with lower spinal rigidity. Mild head lag, no slip-through, variable tone distally. Multiple bilateral contractures: shoulders, wrists with ulnar deviation, finger flexors, jaw, hip flexion, knee flexion, and heel cords. Prominent paraspinous muscles. Fine tremor. Reflexes present. Temperature dysregulation.	Pronounced muscle hypertonia. Kyphosis. Limited passive range of motion. Thoracic rigidity. Tracheostomy, ventilator and feeding tube dependent. She has a bladder catheter. Profuse sweating when excited.
Motor function & strength	Stiff gait marked by hip flexion, thoracic kyphosis, and flexion at the knees. Improvement over time. Strong bilateral grasp. No weakness.	Limited to absent movement. Unable to sit or roll.
Respiration	Neonatal transient hypoxemia. Increased respiratory rate and occasional grunting. Frequent respiratory infections. Hypoxemia and obstructive sleep apnea requiring supplemental oxygen.	Recurrent hypoxic crises in infancy. Tracheostomy and ventilator dependency.
EMG	Suggestive of a generalized myopathy with denervating features. No myotonia or myokymia observed.	No evidence of spontaneous activity or myotonia.
NCS	Sensory responses of the right median and sural nerves were normal. Motor NCS of the right median nerve showed normal distal latency, moderate reduction in response amplitude and normal conduction velocity. Motor NCS of the right peroneal nerve showed normal distal latency, severe reduction in response amplitude, and normal conduction velocity.	Not performed.
Other	CK: 205 U/L. Normal: EEG, brain MRI, and Echo. Negative: *ACTA1, MYH3, TPM2, HSPG2, TNNT3, TNNI2, FKRP, CRYAB,* and microarray.	CK between 200-1,000 U/L. Osteopenia, shortened phalanges, and clinodactyly on X-ray. Normal: brain MRI, EEG and metabolic screening. Negative *ACTA1* and *CRYAB.* Increased echogenicity on muscle ultrasound.